Exaggerated phase–amplitude coupling in the primary motor cortex in Parkinson disease

Coralie de Hemptinne[a,1], Elena S. Ryapolova-Webb[a], Ellen L. Air[b], Paul A. Garcia[c], Kai J. Miller[d], Jeffrey G. Ojemann[e], Jill L. Ostrem[c], Nicholas B. Galifianakis[c], and Philip A. Starr[a,1]

Departments of [a]Neurological Surgery and [c]Neurology, University of California, San Francisco, CA 94143-94115; [b]Department of Neurosurgery, University of Cincinnati College of Medicine, Cincinnati, OH 45267; [d]Department of Neurosurgery, Stanford University, Stanford, CA 94305; and [e]Department of Neurological Surgery, University of Washington, Seattle, WA 98195

Edited by Marcus E. Raichle, Washington University, St. Louis, MO, and approved February 8, 2013 (received for review August 21, 2012)

An important mechanism for large-scale interactions between cortical areas involves coupling between the phase and the amplitude of different brain rhythms. Could basal ganglia disease disrupt this mechanism? We answered this question by analysis of local field potentials recorded from the primary motor cortex (M1) arm area in patients undergoing neurosurgery. In Parkinson disease, coupling between β-phase (13–30 Hz) and γ-amplitude (50–200 Hz) in M1 is exaggerated compared with patients with craniocervical dystonia and humans without a movement disorder. Excessive coupling may be reduced by therapeutic subthalamic nucleus stimulation. Peaks in M1 γ-amplitude are coupled to, and precede, the subthalamic nucleus β-trough. The results prompt a model of the basal ganglia–cortical circuit in Parkinson disease incorporating phase–amplitude interactions and abnormal corticosubthalamic feedback and suggest that M1 local field potentials could be used as a control signal for automated programming of basal ganglia stimulators.

electrocorticography | cross-frequency coupling

Neuronal oscillations, reflecting the synchronized activity of neuronal ensembles, may play an important role in motor and cognitive function. Oscillations may be coupled such that the amplitude of high-frequency activity occurs at a particular phase of a low-frequency rhythm. This phase–amplitude coupling has been observed in several areas of the brain, including the hippocampus, the basal ganglia, and the neocortex (1–9). In neocortex, coupling often occurs between the amplitude of broadband-γ activity (50–200 Hz) and the phase of a variety of low-frequency rhythms, especially δ (5), θ (7, 10, 11), and α (2, 10, 12, 13). The magnitude, preferred phase, and exact frequency bands involved in phase–amplitude coupling are modulated dynamically and with anatomic specificity during performance of a variety of cognitive and sensory tasks (14).

Given its diverse roles in cortical function, there is interest in the possible role of aberrant cross-frequency coupling in neurologic disorders. For example, abnormal synchronization of β- and γ-band activity has been observed in schizophrenia (15). In Parkinson disease (PD), there is mounting evidence for pathological β-band (13–30 Hz) neuronal synchronization in the basal ganglia (16); however, the effects of aberrant basal ganglia activity on cortical function are not fully understood. We hypothesized that, in PD, basal ganglia disease produces abnormal coupling between the phase of the β-rhythm and the amplitude of broadband-γ activity in motor-controlling cortical areas. We tested this hypothesis using a unique approach, adapting the technique of subdural electrocorticography (ECoG) to record local field potentials (LFPs) from primary motor cortex (M1) in patients undergoing deep brain stimulator implantation in the awake state. This technique allowed us to overcome the limitations of the other techniques usually used to investigate cortical oscillatory activity in patients with movement disorders, such as poor source localization (scalp electroencephalography), low signal amplitude with susceptibility to artifact (scalp electroencephalography and magnetoencephalography), and poor temporal resolution (functional MRI). We found excessive β-phase–broadband-γ amplitude coupling in the motor cortex of PD patients compared with subjects with a different movement disorder (primary craniocervical dystonia) and subjects without a movement disorder (patients with medically intractable epilepsy undergoing invasive monitoring). In addition, aberrant coupling was observed between the subthalamic nucleus (STN) and M1 LFPs in PD, and therapeutic deep brain stimulation can reduce abnormal cortical coupling. These findings suggest that aberrant cortical cross-frequency coupling may represent an important mechanism by which abnormal basal ganglia activity disrupts cortical function and impairs normal movement.

Results

We studied 25 subjects with movement disorders (16 PD and 9 primary craniocervical dystonia) undergoing STN deep brain stimulator placement and 9 subjects with epilepsy undergoing invasive monitoring with implanted subcortical grids. Patient clinical characteristics are provided in Table S1. Cortical LFPs were recorded in all subjects, and STN LFPs were recorded in 15 PD patients and 7 of 9 dystonia patients. In all cases, the subdural electrodes covered the arm area of sensorimotor cortex (Fig. S1 and Table S2).

Characteristics of Cortical Phase–Amplitude Coupling in PD. Spectral analyses revealed a peak of oscillatory activity in the β-range (13–30 Hz) in the power spectrum of each patient in all disease states (16). The mean log β-power (13–30 Hz) in M1 did not differ between patient groups (Fig. S2*A*) (Kruskal–Wallis test, $P = 0.19$; PD = 1.7 ± 0.5, dystonia = 1.3 ± 0.5, epilepsy = 1.5 ± 0.4, mean ± SD) (17), motivating a search for more sensitive measures of neuronal synchronization (e.g., a relationship between β-oscillations and population spiking as reflected in broadband-γ activity). Fig. 1*A* illustrates the relationship between β-phase and broadband-γ M1 LFP amplitude for an individual PD patient in an alert resting state (patient PD-8). M1 LFP signals were filtered at different frequencies and aligned on the trough of the β-rhythm (13–30 Hz) (6). Visual inspection of this time–frequency plot revealed an increase in broadband-γ power at the trough of the β-oscillation. β-Phase modulation of signal amplitude is seen over amplitude frequencies from 40 to 400 Hz. Fig. 1*B* shows the index of M1 phase–amplitude coupling computed for the same PD patient over a broad range of frequencies for both phase and amplitude (using a Kullback–Liebler-based mod-

Author contributions: P.A.S. designed research; C.d.H., E.S.R.-W., E.L.A., K.J.M., J.G.O., and P.A.S. performed research; C.d.H. analyzed data; C.d.H. and P.A.S. wrote the paper; P.A.G., J.L.O., and N.B.G. performed patient selection and clinical characterization; and E.L.A., J.G.O., and P.A.S. performed surgeries.

The authors declare no conflict of interest.

This article is a PNAS Direct Submission.

[1]To whom correspondence may be addressed. E-mail: coralie.dehemptinne@ucsf.edu or starrp@neurosurg.ucsf.edu.

This article contains supporting information online at www.pnas.org/lookup/suppl/doi:10.1073/pnas.1214546110/-/DCSupplemental.

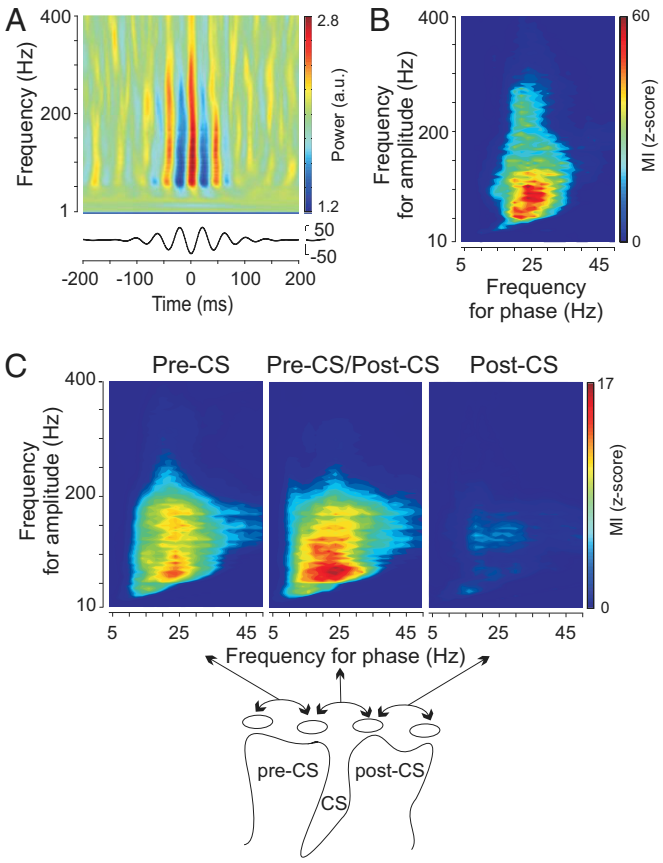

Fig. 1. Examples of phase–amplitude coupling observed in the cortex of PD patients in the alert rest state and the spatial localization of this coupling. (*A*) Scalogram aligned on the β-trough. M1 LFP signals were filtered at different frequencies and aligned on the trough of the β-rhythm (*Lower*; 13–30 Hz). (*B*) Modulation indices over a range of frequencies for phase and amplitude showing a strong coupling between the phase of the β-rhythm and the amplitude of γ-activity (50–300 Hz). The warmest colors represent the strongest coupling. (*C*) Spatial localization of strong phase–amplitude coupling. Each plot shows the averaged modulation indices across all PD patients for particular electrode pairs. (*Upper Left*) Both electrodes anterior to the CS (pre-CS). (*Upper Center*) Electrode pair crossing the CS. (*Upper Right*) Both electrodes located posterior to the CS (post-CS). Schematic representation of the electrode localization relative to the CS is shown in *Lower*.

ulation index expressed as a z score) (6). In this plot, the value of each (x,y) coordinate represents the strength of coupling between the phase of the x frequency and the amplitude of the y frequency. A strong interaction between the phase of the β-rhythm and the amplitude of γ-activity (50–300 Hz) can be observed (warmest color on each graph). Similar patterns of significant cross-frequency coupling (z score > 4.5 for at least one combination of phase and amplitude) were observed in all PD patients (Fig. S2 *B* and *C*). To investigate the cortical localization of coupling, composite modulation index plots were constructed for three contact pairs selected based on their positions relative to central sulcus (CS); the pre-CS, CS, and post-CS pairs. The plots show the average modulation index at each frequency across all PD patients (Fig. 1*C*). Phase–amplitude coupling was the strongest for electrode pairs that have at least one contact over the precentral gyrus. For subsequent grouped analyses in Figs. 2 and 3, either the pre-CS or CS contact pairs were used, depending on which of the two showed the highest phase–amplitude coupling.

Motor Cortex Phase–Amplitude Coupling Is Exaggerated in PD. Averaged M1 modulation index (MI) plots for all patients in each disease group in the alert resting state are shown in Fig. 2*A*. For statistical comparison between groups, the MI of each patient was averaged across the β-band (frequency for phase = 13–30 Hz; frequency for amplitude = 50–200 Hz). The range of frequencies used in averaging is indicated by the white dotted box in Fig. 2*A*, *Left*; this average was called the MI mean. Given the nonnormal distribution of individual subject MI means (P < 0.001 Kolmogorov–Smirnov test), the Kruskal–Wallis test was used to quantify the difference in coupling between diseases (Fig. 2*B*). The magnitude of β-phase–broadband-γ amplitude coupling was much greater in PD patients than subjects with craniocervical dystonia or subjects without a movement disorder (PD = 14.8 ± 10.5, dystonia = 1.2 ± 1.4, epilepsy = 2.0 ± 2.1, mean ± SD; P < 0.001 for Kruskal–Wallis test; P = 0.001 for PD vs. dystonia and P = 0.002 for PD vs. epilepsy). MI plots for each individual subject are provided in Fig. S2 *B–D*. Phase–amplitude coupling observed in dystonia and epilepsy patients was not only smaller but occurred at lower frequencies for phase (PD = 23.1 ± 5.5 Hz, dystonia = 15.3 ± 5.8 Hz, epilepsy = 14.4 ± 6.5 Hz, mean ± SD; P = 0.004 for Kruskal–Wallis test; P = 0.03 for PD vs. dystonia and P = 0.016 for PD vs. epilepsy) as well as a narrower range of phase frequencies. Characteristics of phase–amplitude coupling observed in PD patients are provided in Table S3. Several computational methods are available to quantify phase–amplitude coupling, and several methods are available to rereference the LFP recordings. However, exaggerated cortical phase–amplitude coupling in PD was invariant to the choice of computational or contact referencing method (Fig. S3 *A–E*). Because LFPs in epilepsy patients were recorded from large cortical grids, several contacts covering M1 were available for study, but the findings were invariant to the exact method used to select the M1 contact (Fig. S3 *F* and *G*).

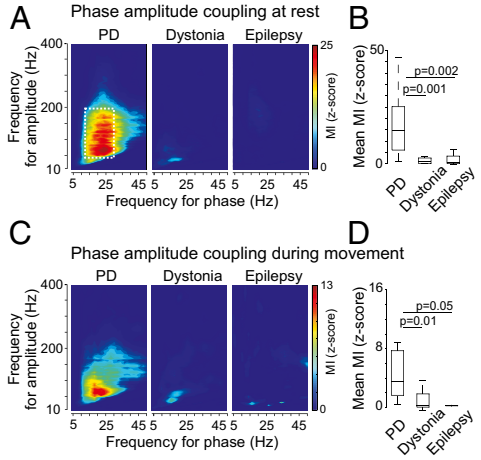

Fig. 2. Comparison of phase–amplitude coupling in the three different disease states. (*A*) Subjects in a state of alert rest. Each plot shows the averaged modulation indices across all patients with the same disease. The white dotted box (*Left*) shows the range of frequencies over which the individual subject modulation indices are averaged to generate the statistical comparisons between groups (*B* and *D*; MI mean) (Fig. 3*F*). (*B*) Box plots showing the stronger phase–amplitude coupling observed in PD compared with craniocervical dystonia and the interictal recordings in epilepsy patients. The horizontal lines represent the medians of the individual subjects' mean MIs (computed over the range shown in *B*); the boxes represent the 25th and 75th percentiles, and the whiskers extend to the most extreme data points not considered outliers (Kruskal–Wallis test, P = 0.001). (*C*) Phase–amplitude coupling in the three different disease states during a movement task. Modulation indices were averaged for all individual subjects within each disease group as in *A*. (*D*) Box plots showing stronger phase–amplitude coupling in PD compared with dystonia and epilepsy (Kruskal–Wallis test, P = 0.006). Medians and ranges calculated as described for *B*.

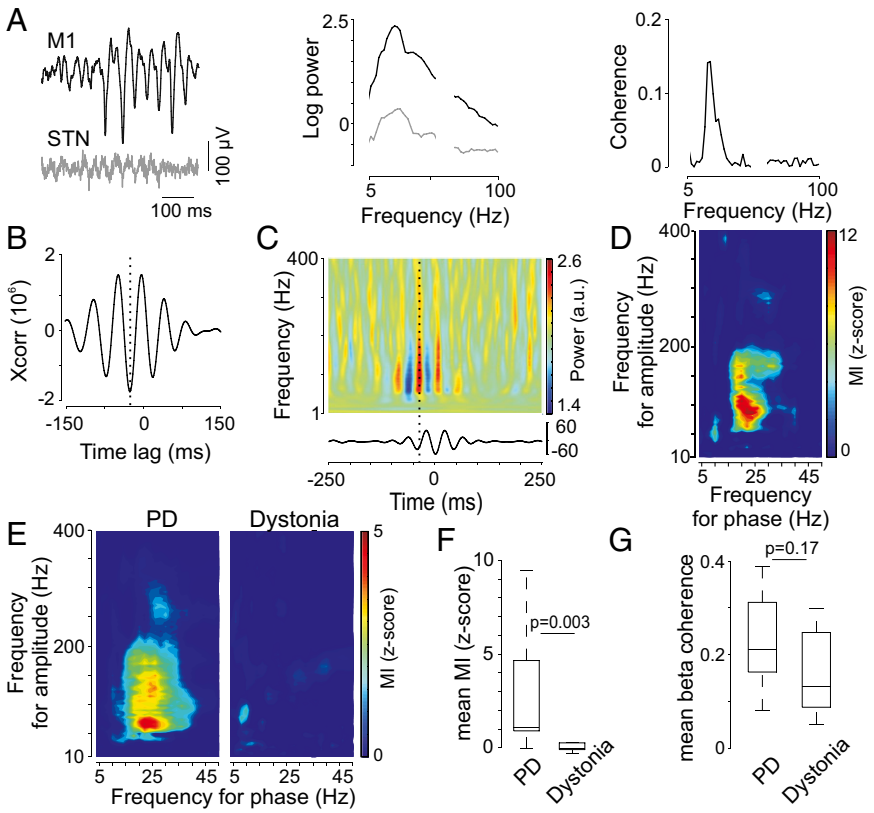

Fig. 3. Cross-structure (STN–M1) interactions. (*A*) Individual examples of STN and M1 LFPs (*Left*), their log power spectral densities (*Center*), and the transformed coherence between both signals (*Right*; PD-4). STN and M1 LFPs are characterized by a peak power spectral density in the β-band and are coherent in this frequency band; 60- and 120-Hz frequencies were removed because of power line noise. (*B*) Cross-correlation between the β-amplitude fluctuations of M1 and STN (PD-4). The cross-correlogram in this example shows M1 β-fluctuations leading STN β-power by 24 ms (vertical dotted line). (*C* and *D*) Example of STN–M1 phase–amplitude coupling plot observed in the same patient. (*C*) M1 scalogram aligned on the β-troughs of the STN LFP. M1 LFP signals were filtered at different frequencies and aligned on the trough of the β-STN rhythm (*Lower*; 13–30 Hz). The black dotted vertical line shows the strongest cortical modulation, which precedes the β-trough by 42 ms. (*D*) The phase and amplitude signals were extracted from STN LFPs and the M1 LFPs, respectively. (*E*) STN–M1 modulation indices were averaged across all PD patients (*Right*) and all dystonia patients (*Left*). (*F*) Box plots showing a significant difference in the phase–amplitude coupling between PD and dystonia (Kruskal–Wallis test, $P = 0.003$). Medians and ranges calculated as described in Fig. 2*B*. (*G*) Box plots showing a nonsignificant difference in the STN–M1 coherence averaged in the β-band (mean β-coherence) between PD and dystonia (Kruskal–Wallis test, $P = 0.17$). Medians and ranges calculated as described in Fig. 2*B*.

We also compared phase–amplitude coupling between subject groups during performance of a simple flexion/extension elbow movement task (Fig. 2*C*). Although the magnitude of phase–amplitude coupling was decreased during the task compared with rest, excessive phase–amplitude coupling during the task in the Parkinsonian state was evident compared with dystonia and epilepsy subjects (Fig. 2*D*) (PD = 6.2 ± 5.9, dystonia = 1.6 ± 3.1, epilepsy = 0.2 ± 0.03, mean ± SD; $P = 0.006$ for Kruskal–Wallace test; $P = 0.01$ for PD vs. dystonia and $P = 0.05$ for PD vs. epilepsy). All subjects were asked to make slow movements that were within the capability of patients with PD, such that movement kinematics during task performance were similar across all groups (Kruskal–Wallis test, $P = 0.7$; angular velocity mean ± SD; PD = 0.81 ± 0.27, dystonia = 0.70 ± 0.2, epilepsy = 0.75 ± 0.2).

Cortical Driving of Basal Ganglia β-Oscillations. Because PD is associated with abnormal neuronal activity in the cortical basal ganglia networks, we investigated the interactions between M1 and STN. Individual examples of STN and M1 signals recorded in a PD patient and their respective log power spectral densities as well as the coherence and temporal correlation of β-power fluctuations between both signals are shown in Fig. 3 *A* and *B*. Analysis of cross-structure phase–amplitude coupling revealed an increase of M1 LFP γ-power occurring at a preferred phase of the STN β-rhythm (13–30 Hz) (Fig. 3*C*). MI plots for STN–M1 coupling are shown in Fig. 3*D* (individual PD example) and Fig. 3*E* (composite plots for all PD and dystonia patients). Cross-structure phase–amplitude coupling was stronger in PD than dystonia (PD = 2.9 ± 2.7, dystonia = 0.1 ± 0.4, mean ± SD, Kruskal–Wallis test, $P = 0.003$) (Fig. 3*F* and Table S3). A significant coupling (z score > 4.5) between STN β-phase and M1 γ-amplitude was found in 11 of 15 PD patients but only 2 of 7 dystonia patients.

In PD, the strongest cortical modulation preceded the STN β-trough by 59 ± 19 ms (mean ± SD; $P < 0.001$ for difference from zero, sign test) (black dashed line in Fig. 3*C*). The finding that the strongest cortical γ-modulation preceded the STN was invariant to the contact referencing method used in STN (Fig. S3 *H* and *I*). Furthermore, cross-correlation of β-power fluctuations (illustrated in Fig. 3*B*) revealed a mean lag time between STN and cortex (over all recordings in PD) of 37.1 ± 26.8 ms, further underscoring the finding that cortical LFP changes precede changes in STN.

Given the strong coupling between M1 β-phase and M1 broadband-γ amplitude, any other brain structure that oscillates coherently with M1 in the β-range would have a statistical relationship between its β-phase and the M1 broadband-γ amplitude without implying a causal connection. However, the magnitude of the STN–M1 coherence did not correlate with the magnitude of the STN phase–M1 amplitude coupling (mean MI, $P = 0.13$; maximum MI, $P = 0.22$). In addition, there was no significant

difference between the mean STN–M1 LFP β-band transformed coherence of PD and dystonia patients, despite the fact that PD patients had much greater cross-structure phase–amplitude coupling (Fig. 3*G*). There was minimal coupling between the phase of M1 LFPs and the amplitude of STN LFPs, showing strong asymmetry in M1–STN phase–amplitude interactions.

STN Phase–STN Amplitude Coupling. Phase–amplitude coupling was also computed using the phase and amplitude of STN LFPs. In eight PD patients, we found a significant interaction between the phase of the β-rhythm and the amplitude of a relatively narrowband high-frequency oscillation (HFO) at >200 Hz (Fig. S4), which has previously been described (18, 19). This pattern of STN–STN phase–amplitude coupling is distinct from β-phase–broadband-γ coupling in that the amplitude frequency over which coupling occurs is both high and narrowband.

Effect of Therapeutic STN Deep Brain Stimulation on Cortical Phase–Amplitude Coupling. In two PD patients, we were able to study acute effects of therapeutic subthalamic deep brain stimulation (DBS) before, during, and after DBS (Fig. 4). Examples of cortical LFPs and their respective power spectral density are shown in Fig. 4*A*. The stimulation artifact was small compared with the biological signal, probably related to the distance between the stimulation and recording sites and the use of bipolar montages. DBS reversibly suppressed exaggerated cortical phase–amplitude coupling (Fig. 4 *B* and *C*). In each example, the suppression of coupling by DBS was partially washed out by 4–5 min poststimulation. The exact time for washin and washout of the DBS effect varied, precluding systematic study of the effect in all subjects because of the time constraints of acute intraoperative recording.

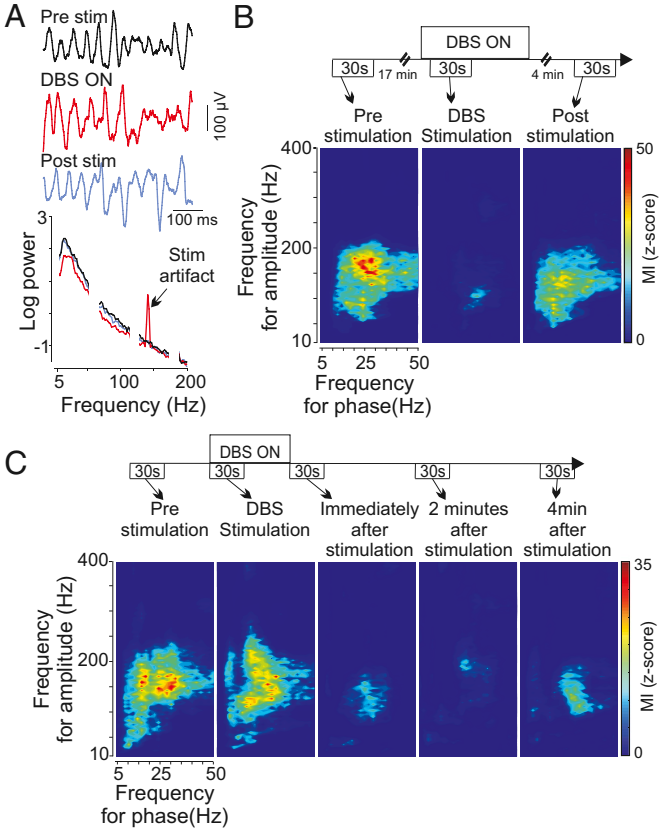

Fig. 4. Examples of the effect of acute therapeutic subthalamic stimulation on phase–amplitude coupling in the resting state. (*A*) Examples of cortical LFPs before, during, and after STN stimulation and their respective log power spectral densities showing minimal stimulation artifact. Black arrow indicates the stimulation artifact at 140 Hz. (*B*) Individual example showing a reduction of phase–amplitude coupling because of acute stimulation (PD-10). This effect had partially washed out by 4 min after cessation of stimulation. *Upper* represents the timeline of the different recordings and the time period selected to compute the phase–amplitude diagrams. Breaks in the timeline indicate an interruption of the recordings. (*C*) Example of a more delayed effect of DBS on phase–amplitude coupling (PD-13). From this continuous recording, five periods have been selected to compute the phase–amplitude coupling as shown by the timeline.

Discussion

In this study, we performed invasive cortical LFP recordings in humans undergoing movement disorders surgery to determine whether rigid–akinetic PD can affect phase–amplitude interactions in the arm area of motor cortex. Similar recordings were obtained in patients with primary craniocervical dystonia who had normal arm function and during the interictal state in epilepsy patients undergoing ECoG for identification of epileptic foci. In addition, simultaneous recordings of cortical and basal ganglia LFPs were performed in patients with movement disorders to study cross-structure, cross-frequency interactions. We had four findings. (*i*) The phase of the β-rhythm (13–30 Hz) modulates the amplitude of broadband-γ in the primary motor cortex. (*ii*) This phase–amplitude coupling is excessive in PD. (*iii*) Cross-structure interactions (STN phase–M1 amplitude coupling) were also high in PD. (*iv*) A potential mechanism for therapeutic deep brain stimulation is reduction of excessive phase–amplitude coupling.

Possible Role of Cortical Phase–Amplitude Coupling in PD Motor Deficits and Implications for Therapy. Coupling between the phase of low-frequency rhythms and the amplitude of high-frequency activity is thought to be a ubiquitous mechanism for the control of many cognitive functions, such as memory, learning, and attention (2, 6–9, 20). The higher-frequency activity (with amplitude that is phase-modulated) may itself be restricted to a relatively narrow-frequency range, or it may involve a very broad spectral band often referred to as broadband-γ (21). The cortical phase–amplitude coupling observed here was of the latter type, consistent with prior studies of interictal LFPs recorded from frontoparietal cortical regions in humans with epilepsy undergoing ECoG (7, 22, 23). Cortical broadband-γ spectral power increases in specific brain areas during performance of motor, visual, language, or cognitive tasks, is correlated with augmentation of the blood–oxygen level-dependent signal measured on functional MRI (24), and is thought to reflect underlying asynchronous spiking activity (25, 26).

In the normal state, the modulation of broadband-γ activity by the phase of low-frequency rhythms is highly dynamic and task- and site-specific (13, 14, 23). Excessive M1 phase–amplitude coupling in PD may reflect a pathological state in which the cortex is restricted to a monotonous pattern of coupling, rendering it less able to respond dynamically to signals from other cortical regions, such as frontal executive areas involved in internally directed movement. Thus, phase locking of cortical broadband-γ activity could be the basis for akinesia, the most fundamental clinical manifestation of PD. Furthermore, because therapeutic DBS can reversibly reduce the strength of the phase–amplitude interaction on a time scale of minutes, the magnitude of cortical phase–amplitude coupling could be used as a control signal for closed-loop therapeutic deep brain stimulation. The ability to detect this signal by a chronic subdural electrode that does not penetrate the cortex has a major advantage over closed-loop paradigms that depend on spike detection (27).

Exaggerated Phase–Amplitude Coupling as the Cortical Manifestation of Increased Basal Ganglia Synchrony. In both PD patients and animal models of parkinsonism, there is growing evidence for

increased synchronization of basal ganglia neurons in the β-frequency range. Simultaneously recorded basal ganglia action potentials are excessively synchronized in the parkinsonian state (28, 29). Basal ganglia spiking in PD is synchronized with the β-phase of STN LFPs (30), and this synchronization is also true of rodent models of parkinsonism (31). Synchronization of basal ganglia spiking is likely to promote a pattern of spike timing in their target cortical areas, in which the probability of spike or spike train occurrence varies rhythmically (27, 32, 33). In cortical LFP recordings, these cortical action potentials are probably detected as a contributor to broadband-γ spectral power (25, 26) and thus, manifested as exaggerated coupling of β-phase to broadband-γ activity, which was observed here.

Circuit Model Emphasizing the Role of Cortical Feedback. The temporal dynamics revealed by simultaneous STN and cortical LFP recordings have implications for the origin of basal ganglia oscillations in PD. Most modeling and experimental work on the origin of excessive basal ganglia β-synchrony has emphasized intrastriatal circuitry (34) or network interactions between intrinsic basal ganglia nuclei, especially STN and external globus pallidus (GPe) (35, 36). Here, by time-averaging cortical activity with respect to the trough of STN β-oscillations, we show that β-modulated waves of cortical broadband-γ precede the STN β-trough by 40–60 ms (Fig. 3*C* and Fig. S3*H*), suggesting an important role for cortical feedback in maintaining pathological basal ganglia oscillations.

A circuit model based on these finding is shown in Fig. 5. Excessive phasic modulation of M1 broadband-γ activity is ideally suited to drive STN activity, because strong phasic inputs to STN are likely to drive STN spiking more efficiently than an asynchronous

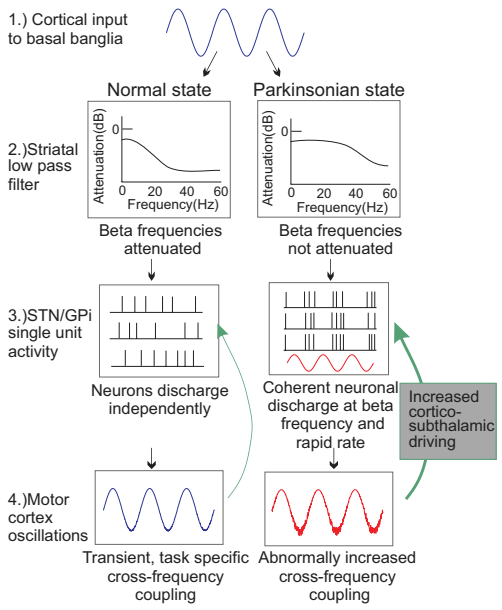

Fig. 5. Model of cortex–basal ganglia interactions in the normal (*Left*) and Parkinsonian (*Right*) states. Part 1: In general, cortical input to the striatum has a strong β-oscillatory component regardless of disease state (41, 42). Part 2: The normal corticostriatal circuitry acts as a low-pass filter with significant β-band attenuation, but the dopamine-denervated striatum produces less β-attenuation (43, 44). Part 3: In the Parkinsonian state, STN and internal globus pallidus (GPi) neurons have excessively synchronized activity in the β-band because of the change in the striatal filter. Part 4: In the Parkinsonian state, excessively coherent basal ganglia β-band neuronal discharge drives M1 to have abnormally increased coupling between β-phase and broadband-γ amplitude. This aberrant coupling, in turn, further strengthens STN β-synchrony and excessive STN firing rate through the hyperdirect corticosubthalamic pathway (green curved arrow) (36–38).

increase in corticosubthalamic activity (36–38). With its emphasis on increased phasic corticosubthalamic driving, our model is consistent with recent theoretical work that emphasizes the imbalance between the corticosubthalamic pathway (hyperdirect pathway) and the intrinsic basal ganglia direct pathway in establishing pathological oscillatory activity (39). In addition, it is supported by recent evidence that STN stimulation antidromically modifies the firing probability of cortical neurons in rodents (33). Optogenetic dissection of basal ganglia pathways in mice also indicates a critical role for the corticosubthalamic pathway in the pathophysiology of Parkinsonism (40) and its successful therapy.

STN Phase–STN Amplitude Coupling Involved Different Frequency Components than Cortical Coupling. Several recent studies have shown phase–amplitude coupling in the STN of PD patients using LFP recordings from externalized STN DBS electrodes several days after surgical implantation (18, 19). Unlike the β-phase–broadband-γ amplitude pattern of cross-frequency coupling that we observed in M1 in this study, in STN, the β-phase–modulated high-frequency activity was a narrowband, very HFO (in the range of 250–350 Hz). Here, we found a similar pattern of HFO coupling in the STN in eight PD patients. The physiological origins of cortical broadband-γ and STN narrowband HFO oscillations are likely different; although the former arises from summed asynchronous spiking activity in neurons with low mean discharge rate, the latter may arise from the organization of STN spikes into synchronized bursts with a very short (3–4 ms) interspike interval within the bursts.

Limitations. Because of the temporal restrictions of human intraoperative studies, we sampled only one brief time epoch (30 s) at limited spatial locations in the off-medication state only. Studies of interictal LFPs in humans with epilepsy recorded with larger 128-channels grids show that, normally, phase–amplitude coupling is present only in a small sample of recordings, and slight changes in behavioral state affect the location and timing of coupling (7, 10, 12, 13). Here, we typically had only one contact covering M1 of movement disorder patients, and we recorded from only a single bipolar pair in STN. Thus, the absence of cross-structure, cross-frequency coupling in 30% of PD patients may be related to low spatial sampling in both structures.

The range of symptom severity in the PD group was small, because mildly affected patients do not undergo DBS implantation; also, the most severely affected patients are less able to cooperate with intraoperative research. This narrow range of symptom severity in our PD patients may explain the absence of correlation between cortical phase–amplitude coupling and disease severity (Fig. S5). Because the dystonia patients had cranial or craniocervical involvement without major arm involvement, it is possible that patients with more generalized dystonia, with arm involvement, could also have abnormal phase–amplitude coupling in arm-related cortical areas. We cannot exclude the possibility that our results reflect compensatory mechanisms in the setting of long disease duration, effects of chronic medication use, or effects of acute medication withdrawal rather than primary mechanisms. However, the strong phase–amplitude coupling in patients who had not been on levodopa therapy for more than 6 mo (Fig. S6) suggests that the findings may be independent of medication use.

Conclusions

PD is characterized by exaggerated coupling between M1 β-phase and broadband-γ amplitude. This excessive coupling is likely to be a cortical manifestation of excessive synchronization in the basal ganglia–thalamocortical circuit, and it may be related to motor dysfunction in PD. Phase–amplitude coupling can be reversibly reduced by therapeutic deep brain stimulation and therefore, could serve as a useful signal for feedback control of implanted devices.

Methods

We studied 25 subjects with movement disorders, 16 PD and 9 primary craniocervical dystonia patients, undergoing STN deep brain stimulator placement. To provide a comparison group of humans without basal ganglia disease, we studied nine subjects with medically intractable epilepsy undergoing invasive monitoring with implanted subcortical grids. Patient clinical characteristics are shown in Table S1. In PD and dystonia patients, cortical LFPs were recorded intraoperatively using a six-contact subdural ECoG strip placed over the primary motor cortex. In epilepsy patients, cortical LFPs were recorded 4–6 d after the surgery using subdural grid arrays covering perirolandic cortex. In all cases, the subdural electrodes covered the arm area of sensorimotor cortex (Table S3). Placement of subdural recording electrodes and STN DBS electrodes is illustrated in Fig. S1. Cortical LFPs were recorded while patients were resting and performing an alternating stop/move task during which they move the arm for 3–5 s and stop the movement for 3–5 s. In 22 patients with movement disorders, STN LFPs were recorded using the DBS electrode. To investigate the effect of STN deep brain stimulation, cortical LFPs were recorded while STN was stimulated. We investigated phase–amplitude coupling within M1 (all subjects), within STN (PD and dystonia patients), and between those two structures (PD and dystonia subjects). All patients gave their written informed consent to participate in this study under a protocol approved by the Institutional Review Board. A detailed description of the methods is provided in *SI Methods*.

ACKNOWLEDGMENTS. We thank Robert Knight, Allison Doupe, Daniel Lim, Srikantan Nagarajan, and Nicole Swann for discussion and critical review of the manuscript. We also thank Leslie Markun for her assistance with clinical data. This work was supported by the National Institutes of Health (Grant R01NS069779).

1. Cohen MX (2008) Assessing transient cross-frequency coupling in EEG data. *J Neurosci Methods* 168(2):494–499.
2. Cohen MX, Elger CE, Fell J (2009) Oscillatory activity and phase-amplitude coupling in the human medial frontal cortex during decision making. *J Cogn Neurosci* 21(2):390–402.
3. Cohen MX, et al. (2009) Good vibrations: Cross-frequency coupling in the human nucleus accumbens during reward processing. *J Cogn Neurosci* 21(5):875–889.
4. Buzsáki G, et al. (2003) Hippocampal network patterns of activity in the mouse. *Neuroscience* 116(1):201–211.
5. Lakatos P, et al. (2005) An oscillatory hierarchy controlling neuronal excitability and stimulus processing in the auditory cortex. *J Neurophysiol* 94(3):1904–1911.
6. Tort AB, et al. (2008) Dynamic cross-frequency couplings of local field potential oscillations in rat striatum and hippocampus during performance of a T-maze task. *Proc Natl Acad Sci USA* 105(51):20517–20522.
7. Canolty RT, et al. (2006) High gamma power is phase-locked to theta oscillations in human neocortex. *Science* 313(5793):1626–1628.
8. Axmacher N, et al. (2010) Cross-frequency coupling supports multi-item working memory in the human hippocampus. *Proc Natl Acad Sci USA* 107(7):3228–3233.
9. Tort AB, Komorowski RW, Manns JR, Kopell NJ, Eichenbaum H (2009) Theta-gamma coupling increases during the learning of item-context associations. *Proc Natl Acad Sci USA* 106(49):20942–20947.
10. Voytek B, et al. (2010) Shifts in gamma phase-amplitude coupling frequency from theta to alpha over posterior cortex during visual tasks. *Front Hum Neurosci* 4:191.
11. Demiralp T, et al. (2007) Gamma amplitudes are coupled to theta phase in human EEG during visual perception. *Int J Psychophysiol* 64(1):24–30.
12. Osipova D, Hermes D, Jensen O (2008) Gamma power is phase-locked to posterior alpha activity. *PLoS One* 3(12):e3990.
13. Yanagisawa T, et al. (2012) Regulation of motor representation by phase-amplitude coupling in the sensorimotor cortex. *J Neurosci* 32(44):15467–15475.
14. Canolty RT, Knight RT (2010) The functional role of cross-frequency coupling. *Trends Cogn Sci* 14(11):506–515.
15. Uhlhaas PJ, Singer W (2010) Abnormal neural oscillations and synchrony in schizophrenia. *Nat Rev Neurosci* 11(2):100–113.
16. Hammond C, Bergman H, Brown P (2007) Pathological synchronization in Parkinson's disease: Networks, models and treatments. *Trends Neurosci* 30(7):357–364.
17. Crowell AL, et al. (2012) Oscillations in sensorimotor cortex in movement disorders: An electrocorticography study. *Brain* 135(Pt 2):615–630.
18. López-Azcárate J, et al. (2010) Coupling between beta and high-frequency activity in the human subthalamic nucleus may be a pathophysiological mechanism in Parkinson's disease. *J Neurosci* 30(19):6667–6677.
19. Özkurt TE, et al. (2011) High frequency oscillations in the subthalamic nucleus: A neurophysiological marker of the motor state in Parkinson's disease. *Exp Neurol* 229(2):324–331.
20. Lakatos P, Karmos G, Mehta AD, Ulbert I, Schroeder CE (2008) Entrainment of neuronal oscillations as a mechanism of attentional selection. *Science* 320(5872):110–113.
21. Crone NE, Miglioretti DL, Gordon B, Lesser RP (1998) Functional mapping of human sensorimotor cortex with electrocorticographic spectral analysis. II. Event-related synchronization in the gamma band. *Brain* 121(Pt 12):2301–2315.
22. Miller KJ, et al. (2010) Dynamic modulation of local population activity by rhythm phase in human occipital cortex during a visual search task. *Front Hum Neurosci* 4:197.
23. Miller KJ, et al. (2012) Human motor cortical activity is selectively phase-entrained on underlying rhythms. *PLoS Comput Biol* 8(9):e1002655.
24. Scheeringa R, et al. (2011) Neuronal dynamics underlying high- and low-frequency EEG oscillations contribute independently to the human BOLD signal. *Neuron* 69(3):572–583.
25. Manning JR, Jacobs J, Fried I, Kahana MJ (2009) Broadband shifts in local field potential power spectra are correlated with single-neuron spiking in humans. *J Neurosci* 29(43):13613–13620.
26. Miller KJ, Sorensen LB, Ojemann JG, den Nijs M (2009) Power-law scaling in the brain surface electric potential. *PLoS Comput Biol* 5(12):e1000609.
27. Rosin B, et al. (2011) Closed-loop deep brain stimulation is superior in ameliorating parkinsonism. *Neuron* 72(2):370–384.
28. Levy R, Hutchison WD, Lozano AM, Dostrovsky JO (2000) High-frequency synchronization of neuronal activity in the subthalamic nucleus of parkinsonian patients with limb tremor. *J Neurosci* 20(20):7766–7775.
29. Nini A, Feingold A, Slovin H, Bergman H (1995) Neurons in the globus pallidus do not show correlated activity in the normal monkey, but phase-locked oscillations appear in the MPTP model of parkinsonism. *J Neurophysiol* 74(4):1800–1805.
30. Moran A, Bergman H, Israel Z, Bar-Gad I (2008) Subthalamic nucleus functional organization revealed by parkinsonian neuronal oscillations and synchrony. *Brain* 131(Pt 12):3395–3409.
31. Mallet N, et al. (2008) Parkinsonian beta oscillations in the external globus pallidus and their relationship with subthalamic nucleus activity. *J Neurosci* 28(52):14245–14258.
32. Pasquereau B, Turner RS (2011) Primary motor cortex of the parkinsonian monkey: Differential effects on the spontaneous activity of pyramidal tract-type neurons. *Cereb Cortex* 21(6):1362–1378.
33. Li Q, et al. (2012) Therapeutic deep brain stimulation in Parkinsonian rats directly influences motor cortex. *Neuron* 76(5):1030–1041.
34. McCarthy MM, et al. (2011) Striatal origin of the pathologic beta oscillations in Parkinson's disease. *Proc Natl Acad Sci USA* 108(28):11620–11625.
35. Bevan MD, Magill PJ, Terman D, Bolam JP, Wilson CJ (2002) Move to the rhythm: Oscillations in the subthalamic nucleus-external globus pallidus network. *Trends Neurosci* 25(10):525–531.
36. Plenz D, Kital ST (1999) A basal ganglia pacemaker formed by the subthalamic nucleus and external globus pallidus. *Nature* 400(6745):677–682.
37. Beurrier C, Congar P, Bioulac B, Hammond C (1999) Subthalamic nucleus neurons switch from single-spike activity to burst-firing mode. *J Neurosci* 19(2):599–609.
38. Bevan MD, Magill PJ, Hallworth NE, Bolam JP, Wilson CJ (2002) Regulation of the timing and pattern of action potential generation in rat subthalamic neurons in vitro by GABA-A IPSPs. *J Neurophysiol* 87(3):1348–1362.
39. Leblois A, Boraud T, Meissner W, Bergman H, Hansel D (2006) Competition between feedback loops underlies normal and pathological dynamics in the basal ganglia. *J Neurosci* 26(13):3567–3583.
40. Gradinaru V, Mogri M, Thompson KR, Henderson JM, Deisseroth K (2009) Optical deconstruction of parkinsonian neural circuitry. *Science* 324(5925):354–359.
41. Crone NE, et al. (1998) Functional mapping of human sensorimotor cortex with electrocorticographic spectral analysis. I. Alpha and beta event-related desynchronization. *Brain* 121(Pt 12):2271–2299.
42. Pfurtscheller G, Aranibar A (1979) Evaluation of event-related desynchronization (ERD) preceding and following voluntary self-paced movement. *Electroencephalogr Clin Neurophysiol* 46(2):138–146.
43. Tseng KY, Kasanetz F, Kargieman L, Riquelme LA, Murer MG (2001) Cortical slow oscillatory activity is reflected in the membrane potential and spike trains of striatal neurons in rats with chronic nigrostriatal lesions. *J Neurosci* 21(16):6430–6439.
44. Weinberger M, Dostrovsky JO (2011) A basis for the pathological oscillations in basal ganglia: The crucial role of dopamine. *Neuroreport* 22(4):151–156.